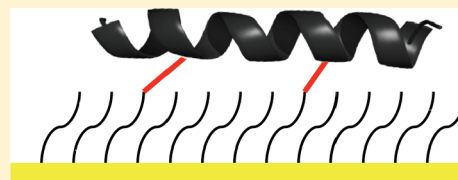


# Demonstration of $\alpha$ -Helical Structure of Peptides Tethered to Gold Surfaces Using Surface Infrared and Circular Dichroic Spectroscopies

Ignacio F. Gallardo and Lauren J. Webb\*

Department of Chemistry and Biochemistry, Center for Nano- and Molecular Science and Technology, and Institute for Cellular and Molecular Biology, The University of Texas at Austin, 1 University Station, A5300, Austin, Texas 78712, United States

**ABSTRACT:** Gold and quartz surfaces terminated in an alkane thiol self-assembled monolayer (SAM) that were partially terminated with azide were reacted with a helical peptide containing two alkyne groups in a Cu(I)-catalyzed Huisgen cycloaddition. Surface grazing incidence angle reflection–absorption infrared spectroscopy (GRAS-IR) was used to determine that when the Au surface was terminated with 25% of the monolayer containing azide groups, 92% of available azide groups reacted with the peptide. The majority of peptides reacted with both alkynes, resulting in peptides tethered to the surface through two covalent bonds. This was confirmed by comparison to a control peptide containing only one reactive alkyne group. Surface circular dichroic (CD) spectroscopy showed that while the helical structure of the peptide was distorted in the reaction solution,  $\alpha$ -helical structure was induced when tethered on the SAM functionalized Au surface. Demonstration of the preservation of desired secondary structure of helical elements at a chemically functionalized surface is an important advance in preparing robust biologically mimetic surfaces to integrate functioning proteins into inorganic materials.



## ■ INTRODUCTION

There is currently great interest in incorporating the biological function of proteins with inorganic substrates and materials for applications in sensing, molecular electronics, biofuels, electrochemistry, proteomics, and beyond.<sup>1,2</sup> While the strategy of integrating biological and inorganic materials has been successfully demonstrated in various antibody and RNA aptamer sensing devices,<sup>3,4</sup> incorporation of proteins onto surfaces for the same purpose has been slower.<sup>5,6</sup> This is largely due to the observation that uncontrolled absorption of a protein on an ill-defined surface often results in loss of the desired protein function because of unfolding, aggregation, improper orientation, or other factors.<sup>7–10</sup> One approach to address this observation is to fabricate chemically functionalized surfaces that replicate biologically relevant protein–protein assembly conditions. If such surfaces could be made to mimic a stable and functional biological interface accurately, an environment that controls the interactions between proteins on a specifically designed substrate could be created. To this end, we are preparing chemically functionalized gold surfaces capable of tethering small peptides to a surface in a reproducible and tunable manner.

In this report, we present the surface functionalization of a helical peptide to a gold surface covered with an azide ( $N_3$ )-terminated self-assembled monolayer (SAM) which has been previously characterized.<sup>11</sup> This functionalization technique results in a substrate in which the surface density of the reactive azide is controlled through the preparation conditions and can be tuned to the structural requirements of the peptide being bound to the surface. The  $N_3$ -terminated surface is then exposed to a helical peptide containing two alkyne functional groups a known distance apart, and through a Cu(I)-catalyzed Huisgen cycloaddition (“click” chemistry), results in a peptide

that is chemically tethered to the surface at two points. By optimizing the azide surface density, the structure of the helical peptide, the distance between the reactive alkyne groups, and the reaction conditions, we have substantially increased reaction yields compared to our previously reported surface-tethered peptides. Using grazing incidence angle reflection–absorption infrared spectroscopy (GRAS-IR) we demonstrate essentially complete reaction between an alkyne-containing peptide and the  $N_3$ -terminated surface for the first time. Furthermore, using surface circular dichroic (CD) spectroscopy, we show that this strategy induces  $\alpha$ -helical structure in the peptide when it is bound to the surface, achieving a chemically fabricated surface with biomimetic structural properties.

## ■ MATERIALS AND METHODS

**A. Surface Preparation.** Peptide-terminated gold surfaces on Si(111) and quartz substrates were prepared as has been described before.<sup>11</sup> Briefly, clean oxidized Si(111) or quartz substrates were covered with 10 nm of Cr followed by 100 nm of Au, then cleaned thoroughly. These substrates were exposed to a solution of 0.25 mM 11-bromo-1-undecane thiol (BrUDT, 99%, Asemblon, Redmond, WA) and 0.75 mM decanethiol (DT, 96%, Sigma Aldrich) in ethanol for 24 h in the dark. After cleaning, these surfaces were immersed in 8 mL of a solution of saturated sodium azide ( $NaN_3$ , Sigma Aldrich) in dimethylformamide (DMF) for 48 h in the dark. Our previous work has shown that this results in a self-assembled monolayer on the Au surface in which 25% of the thiols on the surface are terminated with the azide functional group.<sup>11</sup>

To react the azide-terminated surface with an alkyne-containing peptide through a Huisgen cycloaddition,  $N_3$ -terminated SAMs were immersed in 5 mL solution of 2:1 *t*-butanol/ $H_2O$  containing 166 nmol

Received: August 10, 2011

of the helical peptide LKKLXXKLLKLLKXXLKKL ( $X = \text{prop-argylglycine}$ , PepTech Corp, Burlington, MA), hereafter referred to as  $\alpha 11\text{KL}(\text{CH})$ . Measurements on an energy-minimized structure of this peptide (discussed below) determined that the two alkyne groups were separated by 20 Å and oriented on the same side of the  $\alpha$ -helix. To this solution, 2 mol equiv of  $\text{CuSO}_4$  (Sigma Aldrich), 14 mol equiv of sodium ascorbate (Sigma Aldrich), and 2 mol equiv of tris[(1-benzyl-1H-1,2,3-triazol-4-yl)methyl] amine (TBTA, Sigma Aldrich) were added. This solution was sonicated for 15 min to dissolve the peptide and TBTA, then introduced to the substrate surface. The reaction proceeded for 5 h at 80 °C in the dark in a sealed vessel that had been purged under a flow of  $\text{N}_2(\text{g})$ . Substrates were then rinsed in water followed by ethanol and dried under a stream of  $\text{N}_2(\text{g})$ . Dried samples were stored in the dark.<sup>12</sup>

To determine the extent, if any, of the degradation of the  $\text{N}_3$ -terminated SAM under these reaction conditions, we made a series of control samples exposed to all reaction conditions except any alkyne containing molecule at 23, 55, and 80 °C. At higher temperatures, a peak at  $\sim 2050\text{ cm}^{-1}$  appeared and increased in intensity with increasing temperature. When a surface terminated with 100% DT (i.e., no azide present) was exposed to these reaction conditions at 80 °C, no signal was detected in this region. The peak at  $2050\text{ cm}^{-1}$  has previously been reported as the asymmetric stretching mode of  $\text{N}_3$  complexed to Au.<sup>13</sup> We attribute the appearance of this peak to partial decomposition or distortion of the SAM during the reaction. This provides motivation to further refine our reaction chemistry to avoid high temperatures but, based on the evidence presented below, does not alter our conclusions. Given the increasing use of  $\text{N}_3$ -terminated SAMs on Au for many applications, we suggest that this region be monitored for evidence of SAM damage.

**B. GRAS-IR.** Surface vibrational spectroscopy was collected with a Bruker Vertex 70 Fourier transform infrared (FTIR) spectrometer equipped with a A518/Q horizontal reflection (Bruker) for illuminating the sample at a grazing angle of 80° with respect to the surface normal. The sample chamber was continuously purged with  $\text{N}_2(\text{g})$ , and once inside the chamber samples were transferred with a home-built externally controlled sample manipulation arm to avoid breaking the  $\text{N}_2(\text{g})$  purge. The chamber was continuously purged for 1 h before any measurements to reduce background noise from  $\text{H}_2\text{O}$  and  $\text{CO}_2$ . All measurements were made with p-polarized light. Two sets of scans were collected for each sample. For the first, a mercury cadmium telluride (MCT) detector was used to collect 100 scans between 400 and  $4000\text{ cm}^{-1}$  at a resolution of  $4\text{ cm}^{-1}$ , ideal for the amide carbonyl peaks between 1500 and  $1700\text{ cm}^{-1}$ . For the second, an indium antimonide (InSb) detector was used to collect 100 scans between 1870 and  $4000\text{ cm}^{-1}$  at a resolution of  $4\text{ cm}^{-1}$  to take advantage of its superior sensitivity for the  $\text{N}_3$  absorption near  $2100\text{ cm}^{-1}$ . All samples were referenced to a common clean bare gold substrate to compare absolute differences of all observed signals between different samples. After background subtraction, the baseline of each spectrum was flattened with a linear polynomial function, and the integral under the peak of interest was then computed using the FTIR spectrometer's OPUS software.

**C. Circular Dichroic Spectroscopy.** We are concerned not only with chemically reacting a peptide with the surface, but doing so in a manner that results in a helical structure of the biomolecule. This could be problematic given the reaction takes place in organic solvent (2:1 *t*-butanol: $\text{H}_2\text{O}$ ) and at high temperature (80 °C), both of which could lead to catastrophic distortion of the helix. To test the effect of temperature on this peptide, a solution containing 200  $\mu\text{M}$   $\alpha 11\text{KL}(\text{CH})$  in 2:1 *t*-butanol: $\text{H}_2\text{O}$  was heated from room temperature to 90 °C. Solution CD spectra taken on a Jasco J-815 CD spectrometer illuminating between 200 – 250 nm with a resolution of 1 nm in a 1 mm thick quartz cuvette were collected every 5 °C to measure any peptide conformational changes. Finally, to determine the structure of the peptide once bound to the SAM, surface CD spectra were collected of the peptide-terminated surface. To do this, three peptide-terminated quartz slides were stacked inside a 1 cm quartz cuvette containing Tris buffer. The quartz slides were fixed normal to the CD spectrometer's UV beam with the chemically functionalized

face directed at the UV illumination source. For these measurements 999 scans were collected, which required 13 h of measurement time.<sup>14,15</sup> The background for peptide-terminated spectra was collected on three stacked 25% Br-terminated SAM surfaces on quartz slides inside the same cuvette and immersed in Tris buffer. These background spectra remained qualitatively the same independent of the number of scans (a range of 50–999 scans was explored). All the other instrument parameters were identical to the solution phase CD spectra.

**D. Ellipsometry.** The thickness of the SAMs was determined with a J. A. Woollam M2000 spectroscopic ellipsometer illuminating with broad-spectrum radiation at incident angles of 70° and 75° with respect to the surface normal. To determine the thickness ( $t$ ) of the surface monolayer, only reflections detected at energies between 300 and 600 nm were used. The data were fit to a model consisting of a Si substrate with a layer of Cr 10 nm thick, and a layer of Au 100 nm thick, both of which were fixed. The optical constants for the SAM layer were taken from those of  $\text{C}_2\text{H}_4$  with an initial thickness of 6 nm.<sup>16</sup> The model was not affected by changes in the initial thickness conditions if such changes were less than a few nanometers and as long as the initial condition was larger than the output of the model. The thickness of the monolayer on a given sample was determined from the average of five measurements on different parts of that sample. We report the average of three such samples to determine the thickness of each chemically functionalized surface.

**E. X-ray Photoelectron Spectroscopy.** X-ray photoelectron spectroscopy of all surfaces was conducted on a Kratos Axis Ultra XPS instrument with a monochromatic Al  $K\alpha$  X-ray source illuminating at 1486.5 eV. The ultrahigh vacuum (UHV) chamber was kept below pressures of  $2 \times 10^{-9}$  Torr during sample measurement. Samples were illuminated with a spot  $300 \times 700\text{ }\mu\text{m}^2$  in dimension. High resolution spectra were collected with a pass energy of 20 eV and a resolution of 0.1 eV. All measurements were obtained with the hemispherical electron energy analyzer positioned normal to the sample surface. Peptide-terminated surfaces made from both 25% and 100%  $\text{N}_3$ -terminated surfaces were prepared and measured. The 25%  $\text{N}_3$ -terminated samples provided qualitative proof of the presence of the peptide on the surface at the low concentrations, but the reported values of the N 1s and C 1s peaks were extracted from the 100%  $\text{N}_3$ -terminated peptide functionalized surfaces because of the significantly stronger signal.

## ■ RESULTS AND DISCUSSION

**A. Chemical Characterization of Peptide-Terminated Surfaces.** Representative GRAS-IR spectra of these surfaces are shown in Figure 1. The bottom spectrum in Figure 1 displays a freshly prepared 25%  $\text{N}_3$ -terminated surface, showing only an azide stretching vibration at  $2103\text{ cm}^{-1}$ . To test our reaction conditions, the 25%  $\text{N}_3$ -terminated surface was reacted with ethynylaniline (Figure 1, middle spectrum), resulting in complete loss of the  $\text{N}_3$  peak at  $2103\text{ cm}^{-1}$  and the appearance of the peak at  $\sim 2050\text{ cm}^{-1}$  previously seen in our control reactions.<sup>13</sup> We also observed the emergence of a strong broad feature at  $\sim 1650\text{ cm}^{-1}$ , which has previously been assigned in this molecule as a  $\text{NH}_2$  scissoring mode,  $\nu_c$ .<sup>17</sup> Our control studies demonstrate that these reaction conditions result in complete reaction of the azide with the small molecule, resulting in an ethynylaliline tethered to the surface through a triazole, although with some decomposition of the SAM.

The top spectrum in Figure 1 shows a surface that resulted from exposing a 25%  $\text{N}_3$ -terminated SAM to  $\alpha 11\text{KL}(\text{CH})$  under our reaction conditions. A surface that is 25% terminated in the reactive azide places the azide functional groups approximately 20 Å from each other, based on the alkyl spacing of 5 Å in the thiol.<sup>18</sup> Because the two alkyne groups on an energy-minimized  $\alpha$ -helical structure of this peptide (discussed below) were 20 Å apart, this surface is therefore

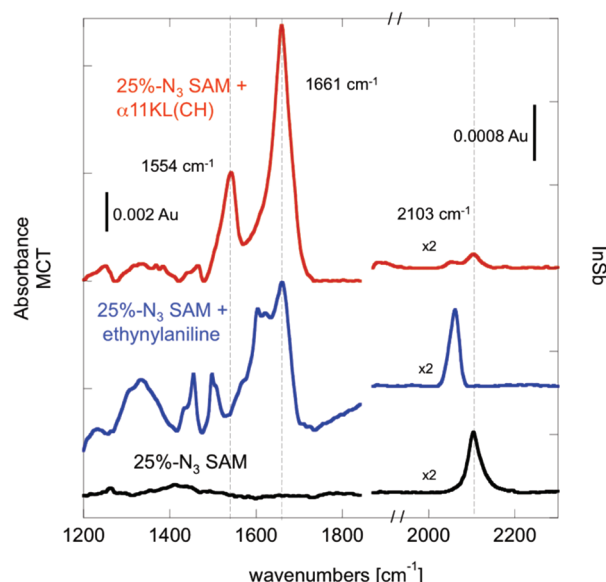


**Figure 1.** Black: GRAS-IR spectrum of a freshly prepared 25%  $N_3$ -terminated surface. Blue: 25%  $N_3$ -terminated surface reacted with ethynylaniline. Red: the product of a 25%  $N_3$ -terminated surface reacted with  $\alpha 11KL(CH)$ . For all spectra, the region from 1200 to 1918  $cm^{-1}$  was measured with a MCT detector (intensities on the left vertical axis), and the region from 1932 to 2300  $cm^{-1}$  was measured with a InSb detector and amplified by a factor of 2 (intensities on the right vertical axis). Scale bars for the intensity of each vertical axis are shown.

tuned to be optimized for maximum reaction between the homogeneously dispersed azide group and the structured  $\alpha$ -helices. A small but measurable peak at 2103  $cm^{-1}$  was observed, indicating that a small amount of  $N_3$  remained on the surface. A small 2050  $cm^{-1}$  band was also present, again indicating some distortion of the azide-terminated SAM at this high temperature. As expected, large amide peaks appeared in the low energy region at 1544 and 1658  $cm^{-1}$ , corresponding to the amide II and I modes, respectively. Because it is possible that a peptide that was not chemically bound to the surface could remain absorbed on the SAM after our reaction, we performed a control experiment in which a 100% DT-terminated surface (i.e., without the reactive azide group) was exposed to the peptide under our reaction conditions, then washed thoroughly according to the procedure described above. Negligible amide peaks were observed on these control surfaces (data not shown), suggesting that there is negligible physical absorption of the peptide on the SAM in the absence of a chemical bond being formed between the peptide and the surface.

To complement the characterization of the  $\alpha 11KL(CH)$ -terminated surfaces, we also collected X-ray photoelectron spectra of 25% and 100% peptide-terminated surfaces. These results are shown in Figure 2. We detected a signal corresponding to the N 1s orbital at 399.8 eV (Figure 2a), which is characteristic of the nitrogen atom in peptide backbone amides.<sup>19</sup> In the C 1s region (Figure 2B), we measured peaks at 284.5, 286, and 288 eV, corresponding to carbon bound to carbon, nitrogen, and oxygen, respectively. These peaks are again characteristic of surface-associated peptides.<sup>20</sup>

We further characterized our surfaces by ellipsometry to monitor the change in overlayer thickness at each step of our

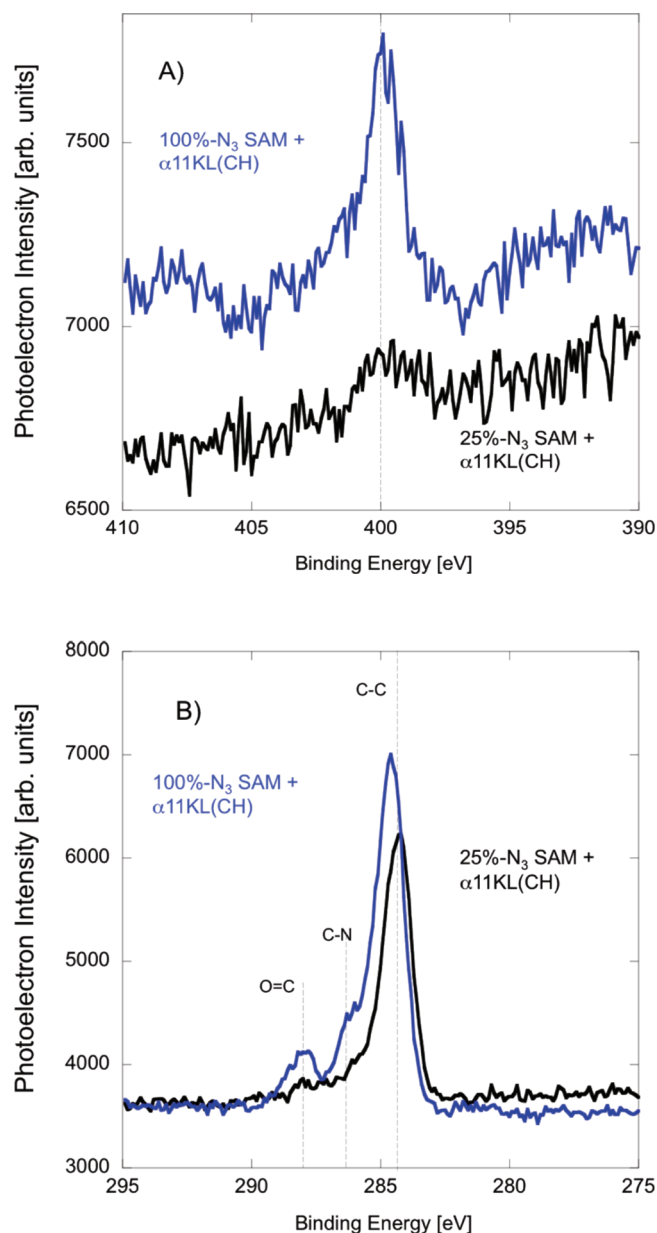


**Figure 2.** XP spectra of the N 1s and C 1s regions of 25% (black) and 100% (blue)  $N_3$ -terminated surfaces reacted with  $\alpha 11KL(CH)$ . (A) N 1s peak measured at 399.8 eV is characteristic of the peptide amino groups. (B) C 1s peaks measured at 284.5, 286, and 288 eV corresponding to the C–C, C–N, and C=O resonances, respectively. Data is shown without any background correction.

surface preparation chemistry. Details on the ellipsometry model and reference thickness of the bare SAM have been published before. In previous work, we found that the sequential addition of the SAM, the  $N_3$ -terminating functional groups, and the peptide resulted in a surface that was  $2.7 \pm 0.2$  nm thick. This agreed well with a simple model of the size of each of these functionalities.<sup>11</sup> New ellipsometry measurements of the  $\alpha 11KL(CH)$ -functionalized surface prepared from 25%  $N_3$ -terminated SAM found that the thickness of the overlayer was  $2.6 \pm 0.1$  nm, in good agreement with our previous measurements and models.

Reaction yields of peptide addition to the  $N_3$ -terminated surface were determined from GRAS-IR spectra by first evaluating the extent of the loss of azide signal in control



**Table 1. Percentage N<sub>3</sub>-Terminated Surface, Reagent Type and Amount, Molar Equivalents of Sodium Ascorbate, CuSO<sub>4</sub>, and TBTA per Reactive Alkyne (CH) for Each Reaction Condition, Huisgen Cycloaddition Reaction Percent Yield, Reaction Time, Temperature and Indication of the Presence and Magnitude of Amide Peaks near 1550 and 1650 cm<sup>-1</sup> on the Sample Surface**

% of N <sub>3</sub> on SAM	reagent type	reagent nmol	CH equiv			reaction yield %	reaction time hours	temperature °C	amide peaks present
			sodium ascorbate	CuSO <sub>4</sub>	TBTA				
25	ethynylaniline	5000	7	1	1	98	20	25	no
25	ethynylaniline	84	7	1	1	86	5	80	no
25	$\alpha$ 11KL(CH)	332	7	1	1	30	20	55	small
25	$\alpha$ 11KL(CH)	166	7	1	1	82	5	80	small
25	$\alpha$ 11KL(CH)	332	7	1	1	92	5	80	large
controls									
25	ethynylaniline	84	7	0	1	0	5	80	no
25	$\alpha$ 11KL(CH)	332	7	0	1	0	5	80	very small
0	$\alpha$ 11KL(CH)	166	7	1	1	0	5	80	very small

samples made by exposing the 25% N<sub>3</sub>-terminated surface to all reaction conditions except the Cu(I) catalyst needed for the cycloaddition. The amount of azide lost in this reaction was attributed to damage to the SAM under these reaction conditions, not triazole formation. Control samples made in this way had the same spectral features as the original 25% N<sub>3</sub>-terminated SAM but a weaker azide signal. The loss in the azide intensity was between 30 and 45% for all control samples, substantially less than our previously reported reaction conditions.<sup>11</sup> All reaction yields were therefore normalized with respect to these controls. When  $\alpha$ 11KL(CH) was reacted with the surface, the extent of the reaction appeared to be directly dependent on the peptide concentration in the reaction solution. As seen in Table 1, reactions with 332 nmol of peptide (664 nmol of CH) resulted in a reaction yield of 92%, but when the peptide concentration was dropped to 166 nmol, the reaction yield dropped to 82%. Higher peptide concentrations did not improve the reaction yield above 92%. This yield is a substantial gain from our previously reported conditions.

**B. Characterization of Surface-Bound Peptide Structure.** To test whether the high temperature of our reaction conditions catastrophically destroyed the helical nature of our peptide, we collected CD spectra of the peptide in a solution of 2:1 *t*-butanol/H<sub>2</sub>O from room temperature to 90 °C and then returned to room temperature. These results are shown in Figure 3. As the temperature increased, the intensity of the molar ellipticity at 208 and 222 nm decreased, indicating that the peptide loses helical structure at high temperature, although the overall line shape of the absorption spectrum remained the same. More importantly, the helicity of the peptide and spectral minima were recovered when the solution was cooled down back to room temperature. Therefore, carrying out this reaction at 80 °C should not disrupt the helical character of the peptide when the substrate is returned to room temperature.

To test the effect of the organic reaction solvent on the structure of the peptide, a solution of  $\alpha$ 11KL(CH) was prepared both in Tris buffer and in 2:1 *t*-butanol/H<sub>2</sub>O, and solution CD spectra were collected of the peptide under both conditions. These spectra are shown in Figure 4, in Tris buffer (black spectrum) and in 2:1 *t*-butanol/H<sub>2</sub>O (the reaction solvent, blue spectrum). In Tris buffer, we measured minima at 207 nm and a second small minima near 220 nm. This peak is quite small and indicates the predominant structure of the peptide is partially unfolded or has assumed a 3<sub>10</sub>-helical structure instead of  $\alpha$ -helix.<sup>21</sup> In a solution of  $\alpha$ 11KL(CH) in 2:1 *t*-butanol/H<sub>2</sub>O (Figure 4, blue spectrum), double minima

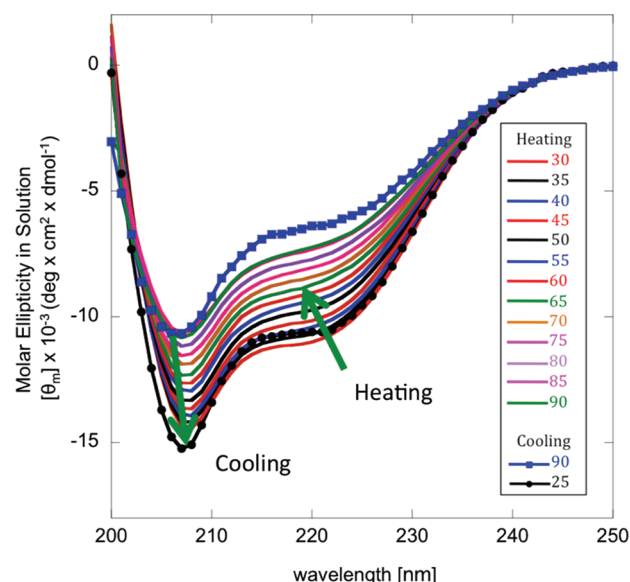


**Figure 3.** CD spectra of  $\alpha$ 11KL(CH) in a solution of 2:1 *t*-butanol/H<sub>2</sub>O from room temperature to 90 °C. In a separate experiment, the solution was cooled from 90 °C (squares) to room temperature (circles), but is shown on the same figure for convenience. Temperatures in °C are listed in the legend. The left vertical axis displays the scale of molar ellipticity of the solution.

observed at 207 and 220 nm were indicative of stronger  $\alpha$ -helical character than when in aqueous buffer. Similar shifts of the ellipticity minimum have been seen previously for peptides in hydrophilic and hydrophobic solvents.<sup>22</sup> Given that 3<sub>10</sub> helices are generally not stable,<sup>23</sup> both of these observations are surprising and are currently being investigated in our laboratory with molecular dynamics simulations.

Finally, to determine the structure of the peptide once bound to the SAM, surface CD spectra were collected of the peptide-terminated surface. As seen in Figure 4 (green spectrum), the CD spectrum demonstrated strong  $\alpha$ -helical structure of the surface-bound peptide, with minima at 209 and 223 nm. Taken together, solution and surface CD measurements demonstrated that while  $\alpha$ 11KL(CH) has weak helical propensity in Tris buffer and in the *t*-butanol/H<sub>2</sub>O reaction solution, it assumes a stable  $\alpha$ -helical structure when tethered to the surface. These results demonstrate a profound structural change imposed on the peptide by chemically binding it to the surface.<sup>24</sup>

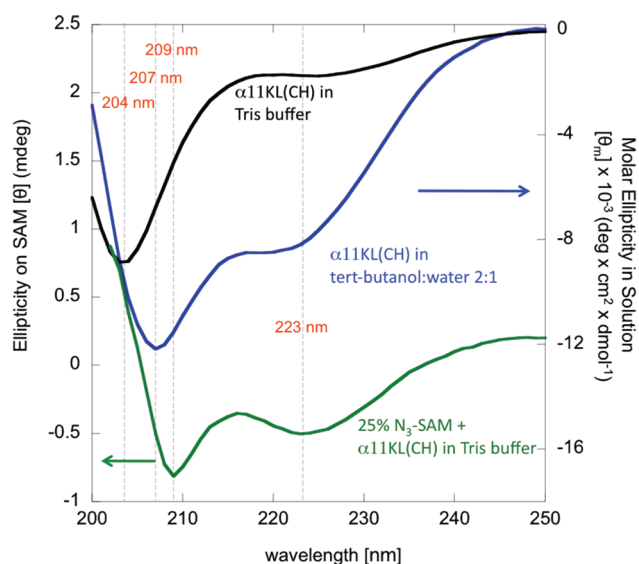


**Figure 4.** CD spectra of  $\alpha 11\text{KL}(\text{CH})$ . Black: peptide dissolved in Tris buffer with minima at 204 and 223 nm. Blue: peptide dissolved in 2:1 *t*-butanol/ $\text{H}_2\text{O}$  with minima at 207 and 220 nm. Green: after reacting  $\alpha 11\text{KL}(\text{CH})$  with a 25%  $\text{N}_3$ -terminated Au surface, showing minima at 209 and 223 nm. The left vertical axis displays ellipticity on the surface, and the right vertical axis displays molar ellipticity in solution. Dashed lines are added to guide the eye.

**C. Orientation of Surface-Bound Helices.** GRAS-IR can be used to calculate the orientation of the peptide's helical axis by measuring the relative intensity of the amide I and II peaks measured at an ordered surface compared with a randomly oriented solution, and from knowing the angle between the peptide backbone and the amide I and II vibrational distortions. This has been described extensively in previous work.<sup>11</sup> From two energy minimized model structures, the angles between the peptide backbone and the amide I mode ( $\theta_{\text{I}}$ ) was determined to be  $22 \pm 5^\circ$  and  $33 \pm 12^\circ$  for the  $\alpha$ -helix and  $3_{10}$ -helix models, respectively. The angles between the backbone and the amide II mode ( $\theta_{\text{II}}$ ) were determined to be  $51 \pm 3^\circ$  and  $52 \pm 12^\circ$  for the  $\alpha$ -helix and  $3_{10}$ -helix models, respectively; the reported error is the standard deviation of all amide bonds in the helix. We collected the FTIR spectrum of the peptide in a solution containing 20 mM  $\alpha 11\text{KL}(\text{CH})$  in Tris buffer dropped on a Au surface and then dried under  $\text{N}_2(\text{g})$ . Collecting the relative intensity of a randomly oriented peptide by GRAS-IR avoids convolution between surface and solution selection rules in our results. The ratio ( $K$ ) of the integrated areas under the amide II and amide I peaks from this randomly oriented peptide was found to be 4.56. With all the above measured parameters for the two helical models, the angle of the backbone of  $\alpha 11\text{KL}(\text{CH})$  with respect to the surface normal was determined to be  $\theta = 60 \pm 5^\circ$  and  $63 \pm 12^\circ$  for the  $\alpha$ -helix and  $3_{10}$ -helix models, respectively.

This angle represents the average orientation of the helical backbone with respect to the surface normal. Our goal is to pin 100% of peptides at the surface through two chemical linkers, resulting in a helical backbone  $\sim 90^\circ$  with respect to the surface normal. To determine the angle that we would measure if 100% of our peptides were linked through only one point, we synthesized an identical peptide containing only one alkyne group (LKKLXKKLLKKLLKKGLKKL, hereafter referred to as  $\alpha\text{KL1x}(\text{CH})$ ). This peptide was also reacted with the 25%  $\text{N}_3$ -terminated surface, and the GRAS-IR spectrum of the resulting

surface is shown in Figure 5. The spectrum of the peptide-terminated surface (black spectrum) clearly shows different

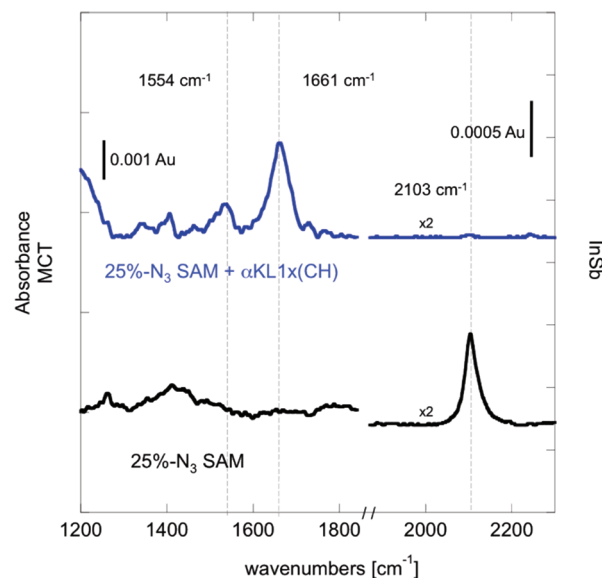


**Figure 5.** Black: GRAS-IR spectrum of a freshly prepared 25%  $\text{N}_3$ -terminated surface. Blue: the product of a 25%  $\text{N}_3$ -terminated surface reacted with  $\alpha\text{KL1x}(\text{CH})$ . For both spectra, the region from 1200 to  $1918\text{ cm}^{-1}$  was measured with a MCT detector (intensities on the left vertical axis), and the high energy region from  $1932$  to  $2300\text{ cm}^{-1}$  was measured with a InSb detector and amplified by a factor of 2 (intensities on the right vertical axis). Scale bars for the intensity of each vertical axis are shown.

relative intensities of the amide I and II modes when compared to the doubly bound peptide in Figure 1. Using the analysis described above, the angle of the backbone of  $\alpha\text{KL1x}(\text{CH})$  with respect to the surface normal was determined to be  $48 \pm 7^\circ$  and  $44 \pm 12^\circ$  for the  $\alpha$ -helix and  $3_{10}$ -helix models, respectively. Angles larger than this that are measured for  $\alpha 11\text{KL}(\text{CH})$  are therefore due to a portion of the surface bound peptide tethered at two points, as intended. Additionally, if the  $\alpha 11\text{KL}(\text{CH})$  peptide is tethered at only one point, the peptide would retain an alkyne functional group. The frequency of this absorption was measured in Tris buffer at  $2123\text{ cm}^{-1}$ , although with small molar absorptivity. We have not detected this peak on peptide-terminated SAM surfaces, even with our InSb detector which has maximum sensitivity in this region. Although this peak will be difficult to measure because of both low absorptivity and surface selection rules, the fact that we consistently do not observe it is evidence that peptides tethered at one point only make up a small portion of the peptide-terminated surface. Although our signal must include peptides tethered with both one and two triazoles, the improvement in both the yield of our reaction conditions and the more ordered peptide from previous reports is impressive. The direct proof from CD spectroscopy that the surface-bound peptide is an  $\alpha$ -helix, not a random coil, makes this an ideal biomimetic surface for a variety of applications.

In conclusion, we have reacted a 25%  $\text{N}_3$ -terminated surface with the peptide  $\alpha 11\text{KL}(\text{CH})$ , resulting in almost complete elimination of the  $\text{N}_3$  stretching mode at  $2103\text{ cm}^{-1}$ . CD spectroscopy has shown that while the helical structure of the peptide is distorted under our reaction conditions, an  $\alpha$ -helical structure is induced when the peptide is tethered to the SAM-

functionalized Au surface. Demonstration of the preservation of secondary structure of helical elements at a chemically functionalized surface is an important advance in preparing robust biologically mimetic surfaces to integrate functioning proteins into inorganic materials. Computational modeling of  $\alpha$ 11KL(CH) under our specific reaction conditions and when chemically bound to the surface is currently underway in our laboratory and is expected to contribute significantly to our understanding of the structure of this molecule when bound to the SAM-functionalized surface.

## AUTHOR INFORMATION

### Corresponding Author

\*E-mail: lwebb@cm.utexas.edu.

## ACKNOWLEDGMENTS

This work was funded by the Army Research Office (Grant No. W911NF-10-1-0280). L.J.W. holds a Career Award at the Scientific Interface from the Burroughs Wellcome Fund. We thank Ms. Michelle Gadush at the Institute for Cell and Molecular Biology at The University of Texas at Austin for peptide synthesis; the Texas Materials Institute for the support of the clean room; and the Texas Institute for Drug and Diagnostic Development (TI3D) Automation Facility for the access to the circular dichroic spectrometer. We also thank the National Science Foundation for funding the Kratos X-ray photoelectron spectrometer (Grant No. 0618242).

## REFERENCES

- (1) Barton, S. C.; Gallaway, J.; Atanassov, P. *Chem. Rev.* **2004**, *104*, 4867–4886.
- (2) Gianese, G.; Rosato, V.; Cleri, F.; Celino, M.; Moreales, P. *J. Phys. Chem. B* **2009**, *113*, 12105–12112.
- (3) Ligler, F. S. *Anal. Chem.* **2009**, *81*, 519–526.
- (4) Taitt, C. R.; Shriver-Lake, L. C.; Ngundi, M. M.; Ligler, F. S. *Sensors* **2008**, *8*, 8361–8377.
- (5) Kulagina, N. V.; Lassman, M. E.; Ligler, F. S.; Taitt, C. R. *Anal. Chem.* **2005**, *77*, 6504–6508.
- (6) Willner, I.; Katz, E. *Angew. Chem., Int. Ed.* **2000**, *39*, 1180–1218.
- (7) Halthur, T. J.; Arnebrant, T.; Macakova, L.; Feiler, A. *Langmuir* **2010**, *26*, 4901–4908.
- (8) Williams, R. A.; Blanch, H. W. *Biosens. Bioelectron.* **1994**, *9*, 159–167.
- (9) Langer, R.; Tirrell, D. A. *Nature* **2004**, *428*, 487–492.
- (10) North, S. H.; Lock, E. H.; King, T. R.; Franek, J. B.; Walton, S. G.; Taitt, C. R. *Anal. Chem.* **2010**, *82*, 406–412.
- (11) Gallardo, I. F.; Webb, L. J. *Langmuir* **2010**, *26*, 18959–18966.
- (12) Dubacheva, G. V.; Van-Der-Heyden, A.; Dumy, P.; Kaftan, O.; Auzély-Velty, R.; Coche-Guerente, L.; Labbé, P. *Langmuir* **2010**, *26*, 13976–13986.
- (13) Partyka, D. V.; Robilotto, T. J.; Updegraff-III, J. B.; Zeller, M.; Hunter, A. D.; Gray, T. G. *Organometallics* **2009**, *28*, 795–801.
- (14) Shimizu, M.; Kobayashi, K.; Morii, H.; Mitsui, K.; Knoll, W.; Nagamune, T. *Biochem. Biophys. Res. Commun.* **2003**, *310*, 606–611.
- (15) Vermeer, A. W. P.; Norde, W. *J. Colloid Interface Sci.* **2000**, *225*, 394–397.
- (16) Palik, E. *Handbook of Optical Constants of Solids II*; Academic Press: 1998.
- (17) Gée, C.; Douin, S.; Crépin, C.; Bréchnignac, P. *Chem. Phys. Lett.* **2001**, *338*, 130–136.
- (18) Ulman, A.; Eilers, J. E.; Tillman, N. *Langmuir* **1989**, *5*, 1147–1152.
- (19) Xiao, S. J.; Textor, M.; Spencer, N. D.; Wieland, M.; Keller, B.; Sigrist, H. *J. Mater. Sci.: Mater. Med.* **1997**, *8*, 867–872.
- (20) Jedlicka, S. S.; Rickus, J. L.; Zemlyanov, D. *J. Phys. Chem. C* **2010**, *114*, 342–344.
- (21) DeGrado, W. F.; Lear, J. D. *J. Am. Chem. Soc.* **1985**, *107*, 7684–7689.
- (22) Gierasch, L. M.; Lacy, J. E.; Thompson, K. F.; Rockwell, A. L.; Watnick, P. I. *Biophys. J.* **1982**, *37*, 275–284.
- (23) Marshall, G. R.; Hodgkin, E. E.; Lings, D. A.; Smith, G. D.; Zabrocki, J.; Leplawy, M. T. *Proc. Natl. Acad. Sci.* **1990**, *87*, 487–491.
- (24) Mandal, H. S.; Kraatz, H. B. *J. Am. Chem. Soc.* **2007**, *129*, 6356–6357.